Estuarine, Coastal and Shelf Science 158 (2015) 1–11

Contents lists available at ScienceDirect

Estuarine, Coastal and Shelf Science

journal homepage: www.elsevier.com/locate/ecss

What processes control the net currents through shallow straits? A review with application to the Bohai Strait, China

Yanfang Li [a, *], Eric Wolanski [b, c], Hua Zhang [a]

[a] Yantai Institute of Coastal Zone Research, Chinese Academy of Sciences, Chunhui Rd 17, Laishan District, Yantai, China
[b] School of Marine and Tropical Biology and TropWATER, James Cook University, Townsville, QLD 4811, Australia
[c] Australian Institute of Marine Science, Cape Ferguson, Townsville, QLD 4810, Australia

ARTICLE INFO

Article history:
Received 8 October 2014
Accepted 7 March 2015
Available online 14 March 2015

Keywords:
straits
flushing
sea level
currents
tides
wind

ABSTRACT

We review the key processes controlling the net water circulation in shallow straits. The circulation is mainly barotropic, driven by the difference in mean sea level and tides on either side of the strait, the wind, the meandering of the currents in the adjoining seas, the bathymetry including the shape and width of the mouths and the presence of narrows, shoals, sills, islands, and lateral embayments. As the oceanography forcing can be non-synchronised on either side of the strait, the resulting net currents through the strait may appear chaotic. We apply these findings to the net circulation through the Bohai Strait in China using local wind, remote-sensing data of currents and sea level, and a hydrodynamic model. The net currents through the Bohai Strait were episodic. They were largest during winter storms when the wind generated a cyclonic coastal current in the northern Yellow Sea that flowed across the width of the Bohai Strait. Like the Luzon Strait, this current meandered and a branch of the current intruded into the northern Bohai Strait along the deeper channel. The wind set-up in the Bohai Sea and the wind-driven longshore current in the southern Bohai Sea generated a seaward flow through the southern Bohai Strait, somewhat like in Irbe Strait. As with the straits of the Seto Inland Sea, stagnation occurred in some embayments. As in the Torres Strait, the islands in the southern Bohai Strait retarded the net flow and increased the width of the outflow zone. These flows were also modulated at very long periods (~60 days) by long waves in the Yellow Sea, possibly generated by meandering of the Kuroshio Current that created an additional sea level slope through the strait. The transit time in the Bohai Strait was 60 and 10 days, respectively, during calm weather and winter storms. The residence time in the Bohai Sea was estimated to be about 1.68 years by the LOICZ model and 1.56 years by the hydrodynamic model, and the influence of the river runoff, including the Yellow River, was negligible.

1. Introduction

A strait is a natural waterway that connects two large bodies of water. There are at least 194 straits in the world (http://en.wikipedia.org/wiki/List_of_straits). Straits are important for the oceanographic circulation in the world and the ecology of oceans and seas and shelf waters because they enable a connectivity between adjoining water bodies. They are important culturally, economically and strategically and, indeed, wars have been fought over them.

It has been 24 years since Pratt (1990) published his book on the physical oceanography of straits. Research on the dynamics of straits has much advanced since that time and the literature is wide and scattered. Thus we first aim to provide a short review of the circulation in straits, focusing on the key processes controlling the net circulation with an emphasis on shallow straits. We then apply these findings to the net circulation in the Bohai Strait in China (Fig. 1). The Bohai Strait separates the Bohai Sea from the Yellow Sea. The Bohai Sea is a relatively flat continental shelf embayment, with an average depth of about 20 m. The strait is 100 km wide and relatively short (~30 km) and has a relative complex bathymetry with several islands in the south; over most of its width the strait is shallow (depth typically less than 20 m) but has a narrow and deep channel (maximum depth ~ 75 m) in the far north of the strait.

Over the past few decades, the water circulation in the Bohai Strait and Bohai Sea has been studied mainly on the basis of numerical models, for which much uncertainty exists because the current meter data needed for model verification are classified and

* Corresponding author.
E-mail address: yfli@yic.ac.cn (Y. Li).

http://dx.doi.org/10.1016/j.ecss.2015.03.013
0272-7714/

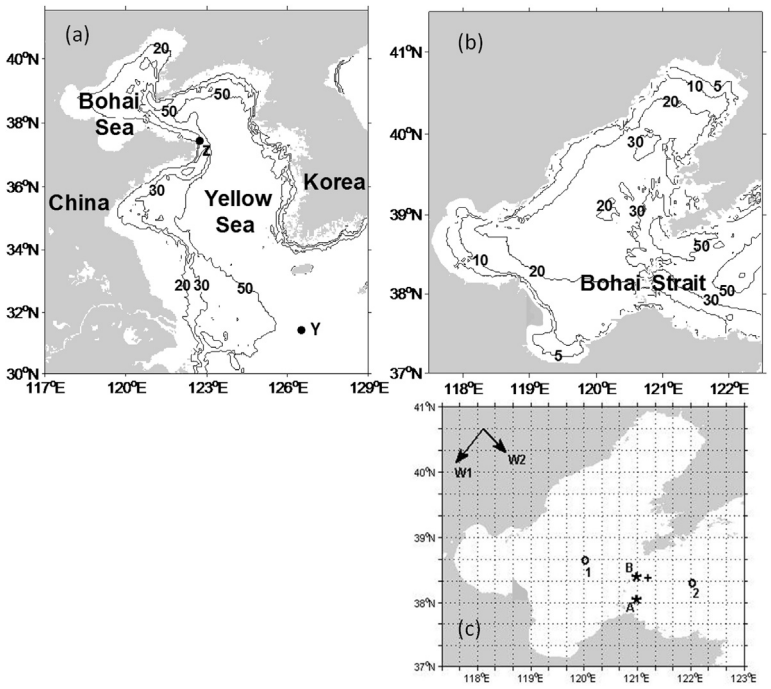

Fig. 1. (a) Location map of the Bohai Sea and Yellow Sea with depth in m (sites Y and Z, labelled black dot). (b) Details of the bathymetry (depth in m) in the Bohai Sea and Bohai Strait. (c) Location map of the site where data were obtained for currents (sites A and B, labelled *), wind (+), and mean sea level (sites 1 and 2, labelled O) around the Bohai Strait.

thus unavailable. From these modeling studies, it was suggested that Yellow Sea waters enter Bohai Strait in the north while Bohai Sea water flows out to the Yellow Sea through the strait in the south (Huang et al., 1999; Fang et al., 2000; Cheng et al., 2004; Hainbucher et al., 2004; Li et al., 2005; Lu et al., 2011; Liu et al., 2012). These models were also used to estimate the residence time in the Bohai Sea. However, these calculations may be sensitive on the value of the horizontal eddy diffusion coefficient, which is unknown a priori. Hainbucher et al. (2004) did not include horizontal eddy diffusion in their ocean mixing model and Liu et al. (2012) chose a value of the horizontal eddy diffusion coefficient to be 15 $m^2\ s^{-1}$. However typical value could be higher, probably of the order of 25 $m^2\ s^{-1}$ (Hrycik et al., 2013) and possibly up to 100 $m^2\ s^{-1}$ especially during storms (Alosairi et al., 2011; Uncles and Torres, 2013).

We studied the net circulation through the Bohai Sea using two methods. Firstly we estimated the residence time in the Bohai Sea using the LOICZ estuarine model. This model is a box model that uses rainfall, runoff, evaporation and salinity data for the Bohai Sea to calculate the actual residence time and bypasses the need for an oceanographic model. We could do that because we had access to a high quality data set. Secondly we used local wind data over the Bohai Sea, remote-sensing data of currents and sea level, and a hydrodynamic model to simulate the dynamics of Bohai Strait. We compared the net circulation through Bohai Strait with that in other shallow straits worldwide. We also estimated the transit time through the Bohai Strait and the average residence time of water in the Bohai Sea.

2. A review of the net water circulation through shallow straits

We review below the processes that control the net currents through straits (Table 1). In long and shallow, straight straits, unidirectional net flows are controlled by the wind, the difference in mean sea level, and bottom friction. In topographically complex long and wide straits, the mean sea level slope and the wind generate a net current but both this net current and the tidal propagation through the strait are impeded by the complex flows generated by the rugged bathymetry. The shape of the entrance to the strait is important so that in wider but short, shallow straits, the wind set-up in the sea can generate an inflow through the strait on one side of the strait and an outflow on the other side. The orientation of the axis of the strait relative to the prevailing currents in the seas is important because for straits oriented parallel to the prevailing oceanic currents, the net currents through the straits depend on the meandering and instabilities of these currents. The mean sea level in the seas on either side of a strait depends on the oceanography of these seas and thus it can be non-synchronised on either side, so that the net currents through the strait also may appear chaotic. In straight straits with stratified waters, the mean sea level slope through the strait generates a net current in the surface layer, while a buoyancy-driven counter-current can prevail in deeper waters. In straits with embayments, eddies form and generate internal doming of the thermocline and inhibit flushing of the bottom waters. In deep straits with sills, topographically controlled large-amplitude internal tides as well as propagating internal waves are generated.

The simplest case is that of long and narrow straits that are shallow enough that the water is vertically well-mixed; the local wind over the strait as well as the different wind-set up in the adjoining seas generate a mean sea level difference (ΔMSL) through the strait, and thus a sea level slope (Fig. 2a). This generates a net current downslope, which is modulated by tides and accelerated by a wind blowing along the downslope direction and decelerated by an opposite wind. This is the case of the Malacca Strait where the net current prevails all year long, but its strength varies seasonally with the seasonal difference of MSL between the Sunda shelf and the West Java Sea to the south and the Andaman Sea to the north (Amiruddin et al., 2011; Rizal et al., 2012). A similar situation prevails in the Strait of Dover, where the net current is correlated with both the difference in sea level between the eastern part of the

Table 1
Classification of straits based on morphology, oceanic and atmospheric forcing, and flow characteristics.

Morphology	Forcing	Flow characteristics	Example	Reference
Long and narrow strait, vertically well-mixed	Large tides, $\triangle$MSL $\neq$ 0.	Strong tidal currents and a net uni-directional flow result; strong recirculating flows occur around shoals.	Malacca Strait; Strait of Dover; Sunda Strait; Singapore Strait; Tatar Strait	Bowden, 1956; Ningshi et al., 2000; Chen et al., 2005; Chong et al., 2005; Pishchal'nik et al., 2010; Amiruddin et al., 2011; Rizal et al., 2012
Shallow strait, vertically well-mixed	Large tidal range comparable to the depth; $\triangle$MSL = 0.	A net current is generated by the tidal asymmetry.	Menai Strait	Harvey, 1968
Long, shallow strait, vertically well-mixed	Numerous sills and shoals; $\triangle$MSL $\neq$ 0.	Friction dissipates the tidal energy, net flows ~0.	Magellan Strait	Medeiros and Kjerfve, 1988
Shallow and narrow strait	Strong tidal currents and the strait facing a wide bay or sea, $\triangle$MSL = 0.	A mushroom jet generates a vortex pair and strong secondary circulation in the sea, and a sink-flow develops when the tides reverse, generating strong tidal mixing.	Nikuchi-Nada	Imasato et al., 1980; Wolanski, 2007;
Narrow strait connecting enclosed seas	ΔMSL ~0, strong tidal currents in the strait, weak currents in the enclosed seas.	The enclosed seas are poorly flushed and separated by well-flushed straits.	Seto Inland Sea	Guo et al., 2004; Chang et al., 2009
Shallow and long strait	Numerous reefs and shoals, $\triangle$MSL $\neq$ 0	Friction and eddies dissipate the tidal energy; small net currents result in vertically well-mixed water; a 2-layer flow occurs for stratified waters; stagnation in some areas and vigorous tidal eddies near reefs and shoals.	Torres Strait for vertically well-mixed waters; Danish Strait for stratified waters	Wolanski et al., 2013; Jakobsen et al., 2010
Wide and shallow strait	Wind and ΔMSL $\neq$ 0 generate a recirculating flow in the adjoining sea.	Bi-directional net currents result with inflow on one side of the strait and outflow in the other side.	Irbe Strait	Sennikovs and Bethers, 2000
Deep strait	Oceanic currents flowing across the width of the strait.	Episodic through-strait currents occur, driven by meandering of the oceanic currents.	Luzon Strait	Chen et al., 2011
Long and deep strait between nearly tideless seas	ΔMSL $\neq$ 0; salinity differences on either side of the strait.	Quasi-steady, two-layer density-stratified flow occur, with opposite currents in the top and bottom layers.	Bosphorus and Dardanelles Straits	Ivanov et al., 1996; Kanarska and Maderich, 2008
Deep, narrow strait	A sill; tides and density difference on either side of the strait.	Highly baroclinic, often unstable, flows develop large amplitude internal waves.	Strait of Gibraltar; Lombok Strait; Strait of Messina	Armi and Farmer, 1985; Bignami and Salusti, 1990 Farmer and Armi, 1999; Cummins, 2000; Hendrawan and Asai, 2011;
Shallow strait but highly stratified waters	A sill, evaporation >> freshwater input from rivers and rainfall.	Modulated by the wind, surface water from one basin flows over the sill to sink in the other basin.	Strait of Hormuz	Pous et al., 2004; Alosairi et al., 2011
Deep sills between ocean basins	Stratification, density difference on either side, ΔMSL $\neq$ 0.	The through-strait flow varies interannually with the El Nino-La Nina cycle; large amplitude internal waves.	Vitiaz Strait	Melet et al., 2013
Shallow strait with islands on one side	Large tides, strong winds, ΔMSL $\neq$ 0 from local wind set-up and far-field oceanic forcing.	Episodic, low-frequency, net through-strait flow occurs with inflow on one side and outflow on the other side.	Bohai Strait	This study.

English Channel and the southern part of the North Sea, and the wind (Bowden, 1956). The shallow Sunda Strait that connects the Java Sea with the Indian Ocean (Ningshi et al., 2000) and the Singapore Strait that connects the Sunda shelf and the West Java Sea (Chen et al., 2005) also have the same situation, even though in both straits there are very strong, reversing tidal currents. Similarly, the net flow in the shallow Tatar Strait that connects the Sea of Okhotsk and the Sea of Japan varies seasonally with ΔMSL and wind (Pishchal'nik et al., 2010).

In very shallow straits the tides alone, in the absence of a ΔMSL, may also generate a net water flux through the strait. This happens in straits such as the Menai Straits (North Wales) (Harvey, 1968), where the sea surface fluctuation is comparable to the depth, and very different in amplitude and phase on either end of the strait. Shallow water frictional effects impede tidal currents during the times when the water depth is much reduced on the end of the strait where the tides are the largest, while this reduction of tidal currents is less pronounced on the end of the strait with smaller tides. This generates a net water flux through the strait even in the absence of a net sea level slope, which is the case in the Menai Straits (Harvey, 1968).

Shoals in shallow straits generate eddies that recirculate water (Fig. 2b), in a similar manner that eddies form in lateral embayments (Fig. 2c); such is the case in Angsa mud bank in Malacca Strait (Chong et al., 2005) where the eddy is also important in retaining prawn larvae. These eddies help dissipate the energy of tidal currents in addition to bottom friction. Additional energy is dissipated by sills and narrows that accelerate the currents and thus increase energy dissipation by bottom friction, so that ultimately in very long, shallow straits, such as in the 500 km long Magellan Strait that connects the Pacific and Atlantic Oceans and separates the South American mainland from the island of Tierra del Fuego. The semi-diurnal tide is rapidly choked as it enters the strait and thus the tidal amplitude along the strait decreases in a step-like manner controlled by the bathymetry, mainly the sills (Medeiros and Kjerfve, 1988).

The bathymetry also generates complex currents within a strait and at its mouth. When swift tidal currents through a narrow strait flow into a wide bay or sea, they form a tidal jet, often called a mushroom jet as it generates a vortex pair (Fig. 2d; Wolanski, 2007). When the tide reverses, the flow resembles a radial flow to a sink if the complex bathymetry permits (Fig. 2d). However,

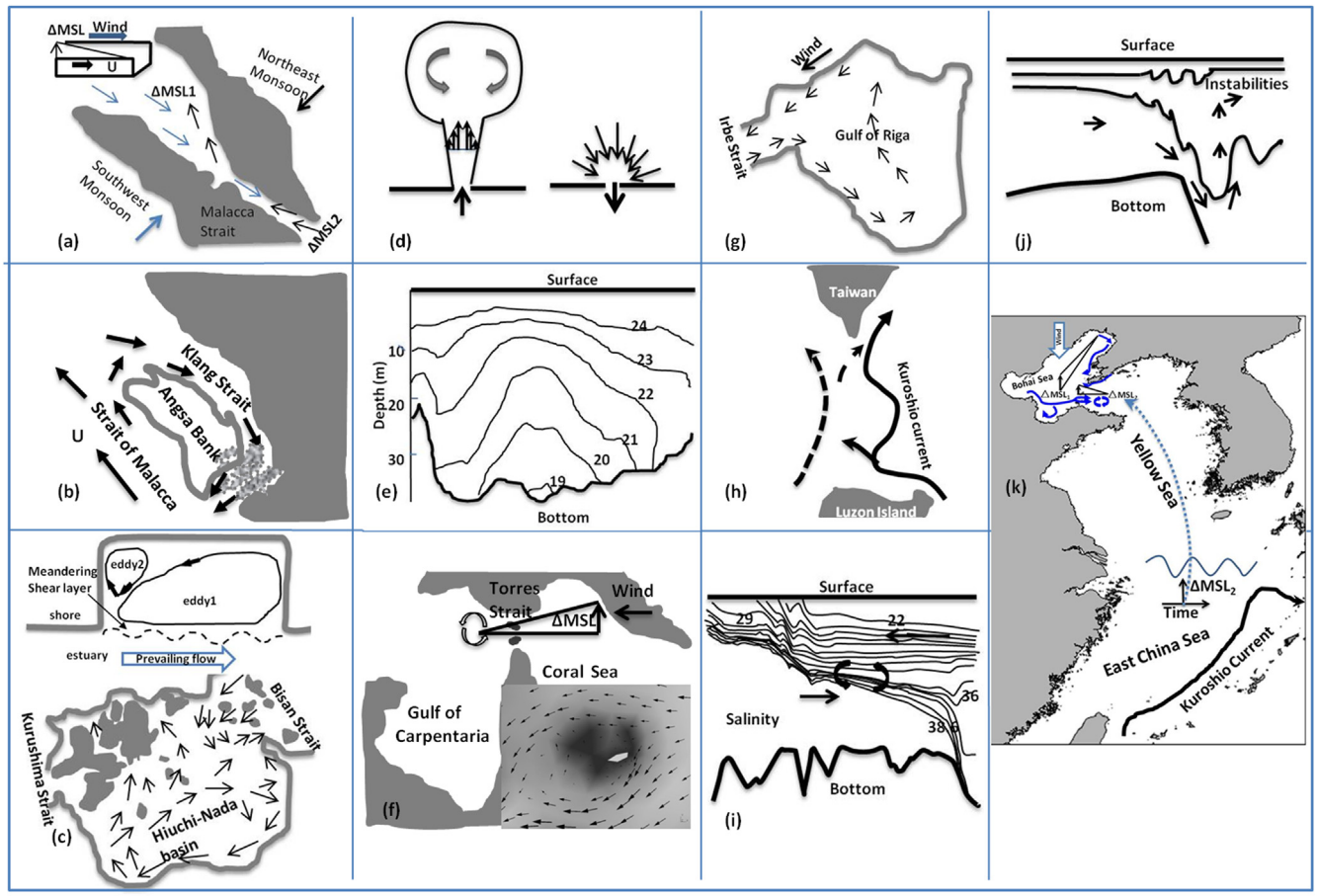

Fig. 2. (a) The net current U in shallow, narrow straits is controlled by the sea level difference ΔMSL and the wind. (b) Secondary currents over shoals in shallow straits, exemplified here in the case of the Strait of Malacca. (c) Eddies and secondary currents are generated in embayments in shallow straits, exemplified for the case of an embayment between two straits in the Seto Inland Sea (simplified from Guo et al., 2004). (d) A mushroom jet is formed when swift tidal currents in a narrow strait enter the sea, and radial flow occurs at the reversing tide. (e) Doming of the isotherms (plotted as σ_t) in an embayment between straits in the Seto Inland Sea (simplified from Chang et al., 2009). (f) The net flow through the reef-studded Torres Strait is determined by the wind and the sea level difference ΔMSL while the complex bathymetry steers the net currents to form zones of net through flow, zones of stagnation, and zones of recirculation. (g) In the shallow and wide Irbe Strait, the wind generates an MSL set-up in the Gulf of Riga together with a recirculating flow that result in an inflow through the strait on one side of the strait and an outflow on the other side (simplified from Sennikovs and Bethers, 2000). (h) Currents through the Luzon Strait are generated by the meandering of the Kuroshio Current (simplified from Chen et al., 2011). (i) Salinity and the estuarine-like water circulation through the Dardanelles Strait (redrawn from Kanarska and Maderich, 2008). (j) Large amplitude lee waves and an internal undular bore form when density stratified waters flow over a sill (adapted from Farmer and Armi, 1999). (k) Sketch of the net circulation through Bohai Strait during winter storms (this study).

when the receiving water has a complex bathymetry, these jets and sink flows are degraded and water meanders along the deeper channel while forming recirculating flows around shoals, headlands and lateral embayments (Imasato et al., 1980). The wind adds complexity to that flow because it generates a downwind current over the shallow water areas and an upwind current in the deeper water. The resulting (tidal-averaged) net currents are very complex and comprise jets, stagnation zones, and eddies, as is shown in Fig. 2c for Hiuchi-Nada, a basin between the Kurushima Strait and the Bisan Strait in the Seto Inland Sea in Japan. In winter the waters in the Seto Inland Sea are vertically well-mixed and the currents near the bottom are smaller than those on the surface due to bottom friction, and these complex flows largely prevail throughout the water column (Guo et al., 2004). As a result the net currents are very small and such waters are flushed very slowly. The flushing rate is even smaller in summer when the water is density-stratified in temperature and salinity. The eddies in such basins (embayments) generate doming of the temperature and salinity isolines (hence of the water density σ_t) (Fig. 2e). The bottom layer basically stagnates and may become anoxic (Chang et al., 2009).

If the strait is shallow, long and studded with numerous reefs, islands and shoals, the complex currents evidenced in the above example of the straits in the Seto Inland Sea are reproduced many times throughout the strait. Such is the case of Torres Strait that connects the Gulf of Carpentaria and the Coral Sea. The net flow through the strait is still determined by wind and sea level difference ΔMSL through the strait (Fig. 2f); the net currents are small and are distributed in a complex maze of slow through flow in some areas, stagnation in other areas, and eddies elsewhere (Fig. 2h; Wolanski et al., 2013).

The net flow through straits also depends on the currents in the surrounding seas. Bidirectional net currents prevail in wide and shallow straits if the water circulation in the adjoining waters generates a mean sea level slope across the mouth of the strait. Such is the case of the wide (30 km) and shallow (depth ~ 20 m) Irbe Strait that connects the Gulf of Riga with the Baltic Sea; wind generates an MSL set-up together with a recirculating flow (Fig. 2g) that results in an inflow through the strait on one side of the strait and an outflow on the other side (Sennikovs and Bethers, 2000).

Currents through deep straits occur when there are strong cross-strait currents in the surrounding seas; such is the case of the

Luzon Strait that connects the Philippine Seas with the Pacific Ocean (Chen et al., 2011). The meandering of the Kuroshio Current on the east side of the strait generates an unsteady bidirectional flow in the strait (Fig. 2h).

Deeper straits are density stratified and the resulting currents are bidirectional, reversing sign with depth in a manner controlled by the barotropic and baroclinic forcings. The simple case is that of relatively straight straits with no sills, such as the Bosphorus and Dardanelles Straits that connect the Black Sea with the Aegean Sea through the Marmara Sea in between. The sea level difference ΔMSL in the Bosphorus Strait is typically 0.2–0.4 m and the salinity difference between the two sides of the strait can be up to 8 ppt; thus swift bidirectional currents result, sketched in Fig. 2i for the Dardanelles Strait (Kanarska and Maderich, 2008). The flow field resembles that in a highly stratified estuary with an outflow of brackish water at the surface and an inflow of high salinity water at the bottom and strong interfacial mixing between the top and bottom layers. Large amplitude (10–20 m) internal waves that may become unstable are also present on the density interface (Ivanov et al., 1996). These internal flows become much more complex and unsteady in the presence of a sill in a stratified strait. Responding to accelerating tidal flows over the sill, instabilities develop in the density interface and these develop into large amplitude lee waves characteristic of an undular jump (Fig. 2j; Farmer and Armi, 1999; Cummins, 2000). Such a hydraulic control by two sills and a narrow width constricting the flows has been documented for the Strait of Gibraltar that connects the Atlantic Ocean with the Mediterranean Sea (Armi and Farmer, 1985) and Lombok Strait that connects the Indonesia Seas with the Indian Ocean (Hendrawan and Asai, 2011). When the tidal current relaxes these sill-generated internal waves can radiate freely away from the sill area for very long distances (e.g. 100 km for the Sulu Sea see the studies by Apel et al., 1985; Hsu and Liu, 2000). All these complex, unsteady flows also have been observed in the Strait of Messina that separates Italy from Sicily (Bignami and Salusti, 1990).

The flow through straits in the presence of a density stratification is further complicated if there are shoals and islands, such as in the Danish Strait that connects the North Sea and the Baltic Sea. As reviewed by Jakobsen et al. (2010) both barotropic and baroclinic exchanges occur through that strait. The barotropic flows are mainly driven by the sea level difference through the strait due to wind set-up and seiche between the Baltic Sea and the North Sea, the tides, and the river inflow to the Baltic Sea. The waters are density stratified mainly in salinity. As in an estuary, the baroclinic transport causes a near surface transport of less saline water from the Baltic Sea to the North Sea and a near bottom transport of more saline water from the North Sea to the Baltic Sea. The flow has hydraulic controls in a number of contractions and sills. The density stratification dampens the turbulence in the water column and it also reduces bottom friction; thus the baroclinic flows modify the net currents (the barotropic flows). The net currents can be predicted from the 1-dimensional laterally-averaged momentum equation, the same equation commonly used in hydraulic flows. This equation balances the terms for the rate of change of hydraulic head, the inertia term, the pressure term, the resistance term and the wind friction term. Basically this equation expresses the balance between water level differences (ΔMSL) and the resistance. The scientifically challenging issue is quantifying the resistance term for barotropic flows in a density-stratified fluid because the resistance term depends on the position of halocline in the water column.

When the sills are sufficiently shallow that they can block the flow in the bottom layer at some stages of the tides but not at other stages, the currents through straits are extremely complicated because the flows in both the top and bottom layers modify their direction and speeds to adjust temporally and spatially to these obstructions (e.g. Cáceres et al., 2006).

Finally, the Strait of Hormuz that separates the Arabian Gulf (also called the Persian Gulf) from the Gulf of Oman is a very special gulf characterised by evaporation far exceeding freshwater input from rivers and rainfall. An inverse estuarine circulation prevails with an inflow at the surface and an outflow at the bottom (Reynolds, 1993). The waters are highly stratified and the effect of the complex bathymetry and the stratification interacting with tidal currents and wind bursting is to generate transient flows comprising eddies, trapping and occasional spills over the sills (e.g. Pous et al., 2004), so that the net currents are very small and the residence time of water commonly exceeds one year (Alosairi et al., 2011).

We have purposely not discussed deep sills between ocean basins because we focused this review on coastal and shelf seas and not on deep seas. However we should mention that these straits can transfer huge amounts of water with flow rate of the order of 1–20 Sv (1 Sv $= 10^6$ m^3 s^{-1}) and they play a vital role in the world-wide circulation of the oceans. This flow through straits varies interannually with the El Nino-La Nina cycle, as has been documented by Melet et al. (2013) for case of Vitiaz Strait that connects the Bismarck Sea with the Salomon Sea.

3. The Bohai Strait

3.1. Methods

We obtained accurate data for the rainfall over the Bohai Sea for the years 2002–2012 from TRMM (Tropical Rainfall Measuring Mission), which was rigorously verified against precipitation data measured at weather stations on islands and along the coast. The runoff data of major rivers (the Yellow, Liaohe, Haihe and Luanhe rivers) flowing into the Bohai Sea were obtained from Water Resources Bulletins of the Ministry of Water Resources of China. The evaporation over the Bohai Sea was estimated using the Objectively Analyzed Air–Sea Fluxes (OAFlux) dataset (Yu and Weller, 2007). We carried out three cruises in the Bohai Sea and Bohai Strait in November 2013, December 2014 and August 2014 that resolved the salinity and temperature structure. The waters were vertically well-mixed in the fall and winter, and in summer a thermocline was present at 20 m in Bohai Strait and the salinity stratification was small (from top to bottom salinity difference of 0.6, not shown). This seasonal thermocline was too deep to intrude into the Bohai Sea. We used all these data of rainfall, salinity, rainfall, evaporation and river runoff in the LOICZ model of Swaney et al. (2011) to calculate the residence time of water in the Bohai Sea.

In the absence of current meter data, we obtained the surface currents at 5-day intervals and at a spatial resolution of 1/3° from Ocean Surface Current Analyses Realtime (OSCAR). High quality data were available for the period from 2007 to 2010. Currents were available for two points (labelled A and B in Fig. 1c) in Bohai Strait; point B was in the central region of the strait, and point A on the south side of the Strait. We also obtained for the same period mean sea level (MSL) data that are merged Topex/Poseidon, Jason and European Remote Sensing sea level anomaly data from ERS-1/2 or Envisat distributed by CLS (Collecte Localisation Satellites) Space Oceanography Division. These data were available at a spatial resolution of 1/3° and 7-day intervals. The various corrections had been applied to the altimeter measurements including ionosphere delay, dry and wet tropospheric correction, electromagnetic bias, solid Earth and ocean tides, ocean tide loading, pole tide, inverted barometer correction, sea state bias and instrumental corrections (see http://www.aviso.oceanobs.com/html). We selected two points (labelled 1 and 2 in Fig. 1c) on either side of the Bohai Strait.

Finally, daily wind data over the Bohai Strait (at the site marked + in Fig. 1c) were provided by Ocean and Sea Ice Satellite Application Facility at a resolution of 1/4°. To coincide with the current data, wind data were averaged over 5 days. The wind vectors were resolved along the longest axis of the Bohai Sea (W_1, across strait, Fig. 1c), and the other direction was through strait (W_2).

As the data from our research cruises demonstrated that the waters were well-mixed in the Bohai Sea and Bohai Strait in winter and autumn, we modeled the water circulation in the model domain shown in Fig. 1b using the 2D model of Brinkman et al. (2002). The model was forced at the Yellow Sea open boundary by tides, observed MSL at site 2 (assume to occur throughout the width of the Bohai Strait open boundary), and wind. The mesh size was 7.5 km, and the model runs lasted 120 days. The model was verified (not shown) for the tides in the Bohai Sea against the findings of Hainbucher et al. (2004).

To calculate the residence time of water in the Bohai Sea and the transit time through Bohai Strait, waterborne particles were released throughout the model domain and their trajectories were tracked by the advection-diffusion model of Spagnol et al. (2002). This was done for several scenarios listed in Table 2, in order to evaluate, based on the measured wind and MSL data, the relative influence of storms, long waves in the Yellow Sea, and various assumptions on the value of the eddy diffusion coefficient K_x.

3.2. Results

3.2.1. Observations

The mean sea level (MSL) on both sides of the strait (MSL1 and MSL2) fluctuated in time with maximum range of 0.6 m (Fig. 3a). Both MSL1 and MSL2 were energetic at periods between 40 and 90 days while MSL2 in the Yellow Sea also was energetic at shorter periods (Fig. 4a). The wind fluctuated seasonally and there were particularly strong southerly winds in winter (Fig. 3b). The wind was most energetic at higher frequencies (<20 days) and the remaining spectra peaks were significantly smaller (Fig. 4b). The currents were mostly positive (i.e. an outflow from the Bohai Sea into the Yellow Sea) peaking at about 0.25 m s^{-1} (Fig. 3c). The currents at sites A and B were similar and were energetic at the same long periods as the energy peaks of MSL1 and MSL2.

The through-straits currents and the difference in MSL (ΔMSL = MSL1-MSL2) through Bohai Strait were highly coherent (C_o^2, Fig. 5a) with a small phase lag of less than 45° (i.e. less than a few days, Fig. 5b). There was no significant coherence ($C_o^2 < 0.3$) between the through straits currents and either one of the wind components W_1 (across strait) and W_2 (through strait).

The altimetry data revealed strong net across-strait currents during winter storms in the Bohai Strait (Fig. 6). Much smaller net currents prevailed during the rest of the year (not shown). The long waves in the northern region of the Yellow Sea were made apparent by low-frequency MSL fluctuations of up to 0.3 m (sites 2 and Z in Fig. 3a and 7e). There were also low-frequency MSL fluctuations of up to 0.2 m in the southern Yellow Sea/East China Sea (Fig. 7e for site Y); and thus it appears that the MSL fluctuations in the northern Yellow Sea at the lowest frequencies were due to MSL fluctuations in the East China Sea (Fig. 7). These MSL fluctuations modulated the net flows through the Bohai Strait. These long waves were used as input as open boundary data to the model. Separately to the effect of storms illustrated in Fig. 6, generally Yellow Sea water entered the Bohai Sea through Bohai Strait during rising MSL in the East China Sea (and such events can last several months as is shown in Fig. 7), and Bohai Sea water exited through Bohai Strait at falling MSL in the East China Sea (not shown).

3.2.2. Predictions

The average rainfall and evaporation over the Bohai Sea during 2002–2012 were 0.76 and 0.9 m a^{-1}, respectively. The average runoff from all rivers flowing in the Bohai Sea during 2002–2012 was 3.84×10^{10} m^3 a^{-1}. The average salinity in the Bohai Sea and in the Bohai Strait was 29.92 and 30.87, respectively. For a surface area of 7.7×10^{10} m^2 and a mean depth of about 20 m, the LOICZ estuarine model (Swaney et al., 2011) predicts the residence time of Bohai Sea water to be 1.68 years.

Examples of the predicted net currents are shown in Fig. 8 for two scenarios (scenario 1 for tides only and 7 for a winter storm, Table 2). For scenario 1, the residual currents in the Bohai Strait were very small, of the order of a few cm s^{-1} (Fig. 8a). For scenario 7, the predicted net current through the Bohai Strait was eastward (from the Bohai Sea to the Yellow Sea, Fig. 8b) in the southern region with values of ~0.25 m s^{-1} in agreement with our current data (Fig. 3c). This was balanced by a narrow jet-like inflow in the northern region with smaller current speeds in view of the larger depths. It takes time for these through-strait currents to be fully established following a sea slope generated by wind set-up in the Bohai Sea and the long waves from the East China Sea; thus there were lags between the currents and sea level slope (Fig. 5b); at the highest frequencies (25–40 days) where the values of C_o^2 were the largest, the currents lagged the sea level slope; at lower frequencies (40–70 days) where the values of C_o^2 were much smaller, the sea level slope lagged behind the currents. In all cases except for NE storms, the predicted net current off the mouth of the Yellow River was longshore eastward (e.g. Fig. 8b), being typically ~0.02–0.03 m s^{-1} in calm weather and <0.1 m s^{-1} during storms, in agreement with the observations of Liu et al. (2012) and Wang et al. (2014).

The percentage of Bohai Sea waters remaining in the Bohai Sea after 120 days subject to the scenarios (1–7) and mixing coefficients (A, B, C) described in Table 2 are shown in Table 3. That percentage varied between 63.4 and 91.6 (mean = 80.4 ± 8.5). A few are plotted in Fig. 9. Exponential curves were fitted to these 120 days trend lines to estimate the e-folding time, i.e. the residence time, which is shown in Table 3. That predicted residence time varied between 0.60 and 3.12 years (mean = 1.56years ± 0.8). The mean residence time (1.56 years) predicted by the hydrodynamics model compares favorably with the residence time (1.68 years) predicted by the LOICZ model. The tides contributed very little to the flushing. The wind had a dominant effect, particularly winter

Table 2
Characteristics of the seven scenarios to predict the water circulation in the Bohai Strait. For each of these seven scenarios, the flushing of the Bohai Sea was estimated using three values (A, B, C) of the horizontal eddy diffusion coefficient K_x (m^2 s^{-1}).

Scenario	A	B	C
Scenario 1: 0 wind, 0 long waves, tides	15	25	100
Scenario 2: NE storm winds; 0 long waves, tides	15	25	100
Scenario 3: 0 wind, long waves in the Yellow Sea, tides	15	25	100
Scenario 4: NE storm winds, long waves in the Yellow Sea, tides	15	25	100
Scenario 5: N storm winds, long waves in Yellow Sea, tides	15	25	100
Scenario 6: N storm winds, 0 long waves in Yellow Sea, tides	15	25	100
Scenario 7: NW storm winds, long waves in Yellow Sea, tides	15	25	100

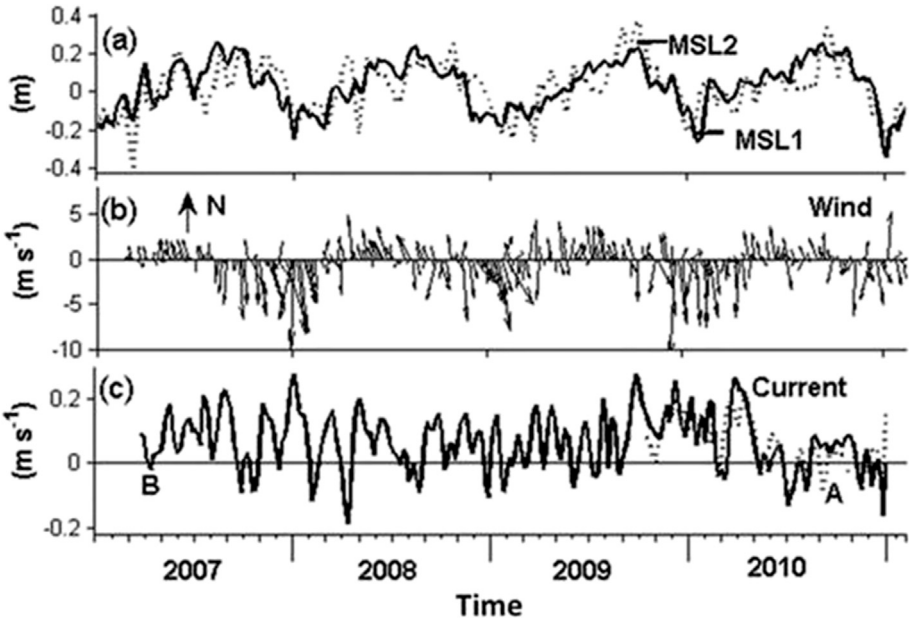

Fig. 3. Time-series plot of observed MSL, wind, and surface currents in the Bohai Strait (positive for an outflow from the Bohai Sea to the Yellow Sea).

storms, and the long waves in the Yellow Sea increased the flushing rate by about 50%.

The transit time of Bohai Sea water through the Bohai Strait was calculated by seeding only in the Bohai Sea and using the hydrodynamic model to estimate the time for the particles to start to enter the Yellow Sea. That transit time was about 60 days in calm weather and with no long waves in the Yellow Sea (See Scenario 1C in Fig. 9 for seeding in the Bohai Sea only), 30 days during storms

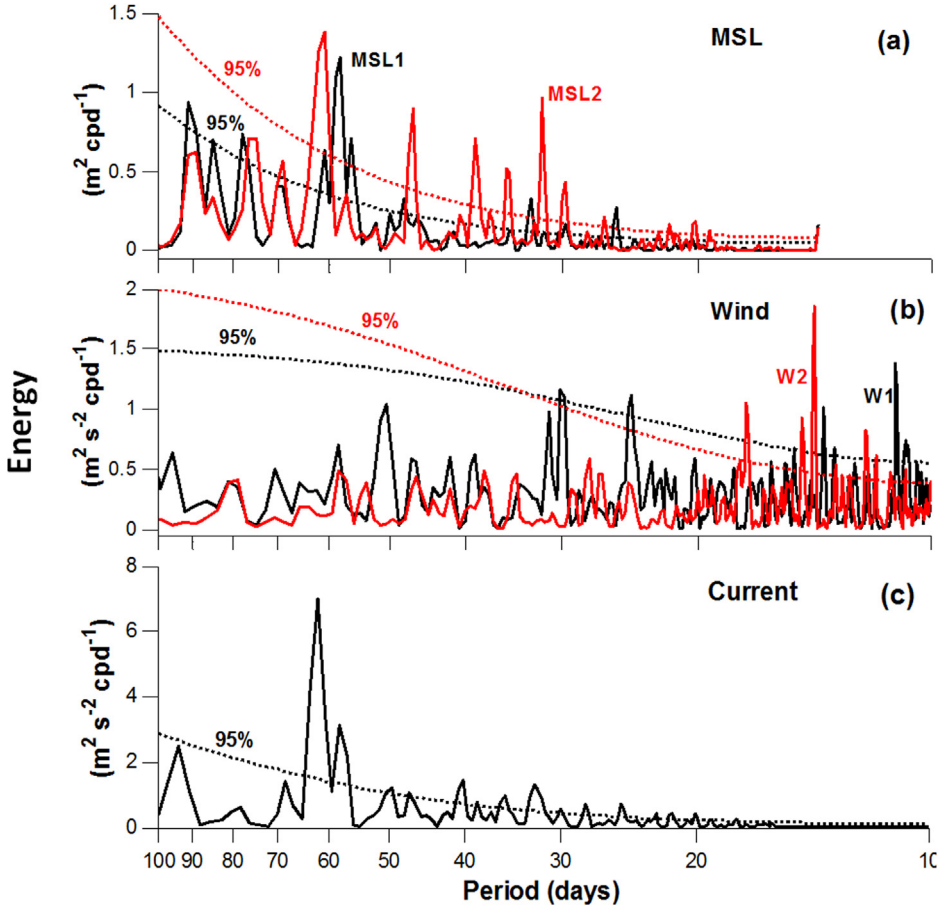

Fig. 4. Power spectra of MSL, surface current and wind (the dashed lines are the 95% significance level).

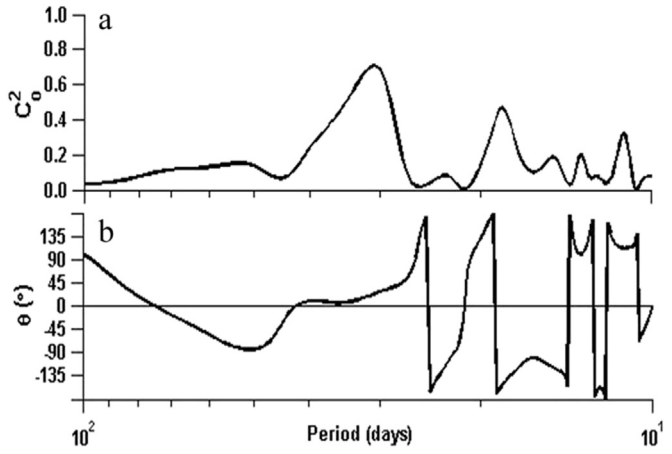

Fig. 5. Coherence squared (C_o^2) and phase ($\theta > 0$, which means MSL slope leads before currents) relationship between MSL slope across the Strait and surface current at station B.

and with no long waves in the Yellow Sea, and 10 days during storms and with long waves in the Yellow Sea (not shown).

4. Discussion

The results for the Bohai Strait show that the system is sensitive to the circulation in the Bohai Sea, in the Yellow Sea and the East China Sea, to the bathymetry in the strait, and to wind. To verify this prediction we characterized the net circulation through the Bohai Strait, China, using the LOICZ estuarine flushing model as well as current, sea level and wind data combined with a hydrodynamic model. The renewal time of water in the Bohai Sea was predicted to be 1.68 years. This estimate is robust and implicitly takes into account the return coefficient (i.e. the fraction of the water that leaves the Bohai Sea once but returns later on) because it is based on calculations of the net budget of salt from field data; it is best interpreted as the exposure time (i.e. Andutta et al., 2014). This may explain why our estimate of 1.68 years is larger than the estimate by Hainbucher et al. (2004) of the turnover time (the time it takes for the water to leave for the first time, ignoring the fact that it may return later) of 0.5–1 year.

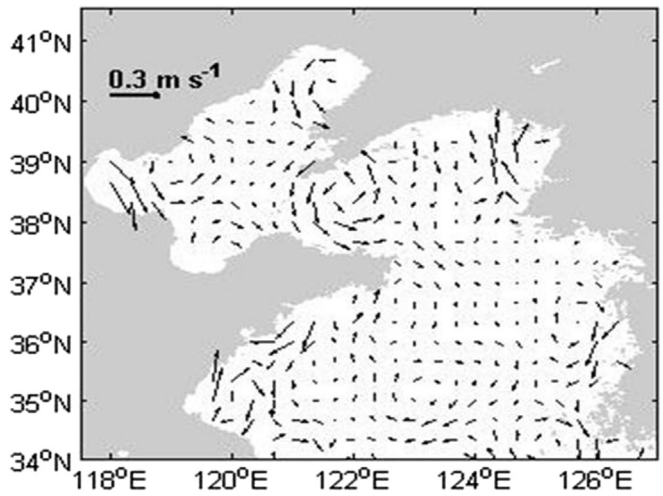

Fig. 6. Observed net surface current in the Yellow and Bohai Sea averaged for the period 1–21 January, 2014.

Our current and sea level data in the Bohai Strait are the first data used to quantify the net currents through Bohai Strait. The mean sea level difference (ΔMSL) through the strait was energetic at low frequencies, and the current data show a net outflow in the southern 2/3 of the straits and that was coherent at those low frequencies with ΔMSL through the strait. Peak currents were about 0.25 m s^{-1}. The wind also had low-frequency fluctuations but much of the energy occurred at somewhat higher frequencies.

The low frequency mean sea level in the northern Yellow Sea was not coherent with the wind, suggesting that much of the mean sea level fluctuations were not due to locally generated events. Indeed we found mean sea level fluctuations of up to 0.2 m peak to trough at the mouth of the southern Yellow Sea facing the East China Sea. We suggest that some of these events may be due to the meandering of the Kuroshio Current in the China Sea generating long waves that propagate into the Yellow Sea (Qiu et al., 1990; Kimura and Sugimoto, 2000).

A sensitivity analysis using the hydrodynamic model suggests that the tides alone generated negligible net currents through the Bohai Strait and that the currents through the Bohai Strait were driven by events. They were the largest during winter storms and modulated by the propagation of long waves in the Yellow Sea. They reversed direction during northeasterly (NE) storm winds.

The flushing of the Bohai Sea was thus episodic. It was the slowest during calm weather and for no long waves in the Yellow Sea (Fig. 9, Table 3), and the transit time of Bohai Sea water through Bohai Strait was then about 60 days. Flushing was fastest during winter storms, particularly for northwesterly (NW) winds, when the transit time through the Bohai Strait was about 10 days. However, flushing could stop entirely during NE winds. The assumption on the value of the horizontal eddy diffusion coefficient also influenced the estimates of the flushing rate. As shown in Table 3, during calm weather higher values of the eddy diffusion coefficient resulted in increasing the flushing rate; this was due to the increased diffusion through the strait to reach the open boundary of the Yellow Sea. However during winter storms increasing values of the horizontal eddy diffusion coefficient reduced the flushing rate; this was due to diffusion transferring particles from the export zone in the south of Bohai Strait to the import zone in the north.

During an episodic event with an outflowing current of 0.2 m s^{-1} in the southern Bohai Strait, the outflowing flow through Bohai Strait was about 300,000 m^3 s^{-1} and this was orders of magnitude larger than the peak discharge of the rivers flowing into the Bohai Sea, including the Yellow River. Thus the river runoff had a negligible influence on the net currents through Bohai Strait.

The currents through the Bohai Strait fluctuated constantly in response to the wind set-up and the wind-generated coastal currents in the Bohai Sea and in the Yellow Sea, and to long waves in the Yellow Sea. The residence time of water in the Bohai Sea was thus the result of integrating over time the various episodic events generating currents through Bohai Strait.

5. Conclusion

We studied the net circulation through the Bohai Sea using two methods. Firstly, the renewal time in the Bohai Sea was estimated to be 1.68 years using the LOICZ estuarine model. The influence of the river runoff, including the Yellow River, was negligible.

Secondly we used local wind data over the Bohai Sea, remote-sensing data of currents and sea level, and a hydrodynamic model to model the dynamics of the Bohai Strait. We found that the net circulation through the Bohai Strait is controlled (Fig. 2k) by both the cyclonic circulation and long waves in the Yellow Sea, local wind and especially winter storms that generate a wind set-up in the Bohai Sea, as well as low-frequency (periods typically > 90

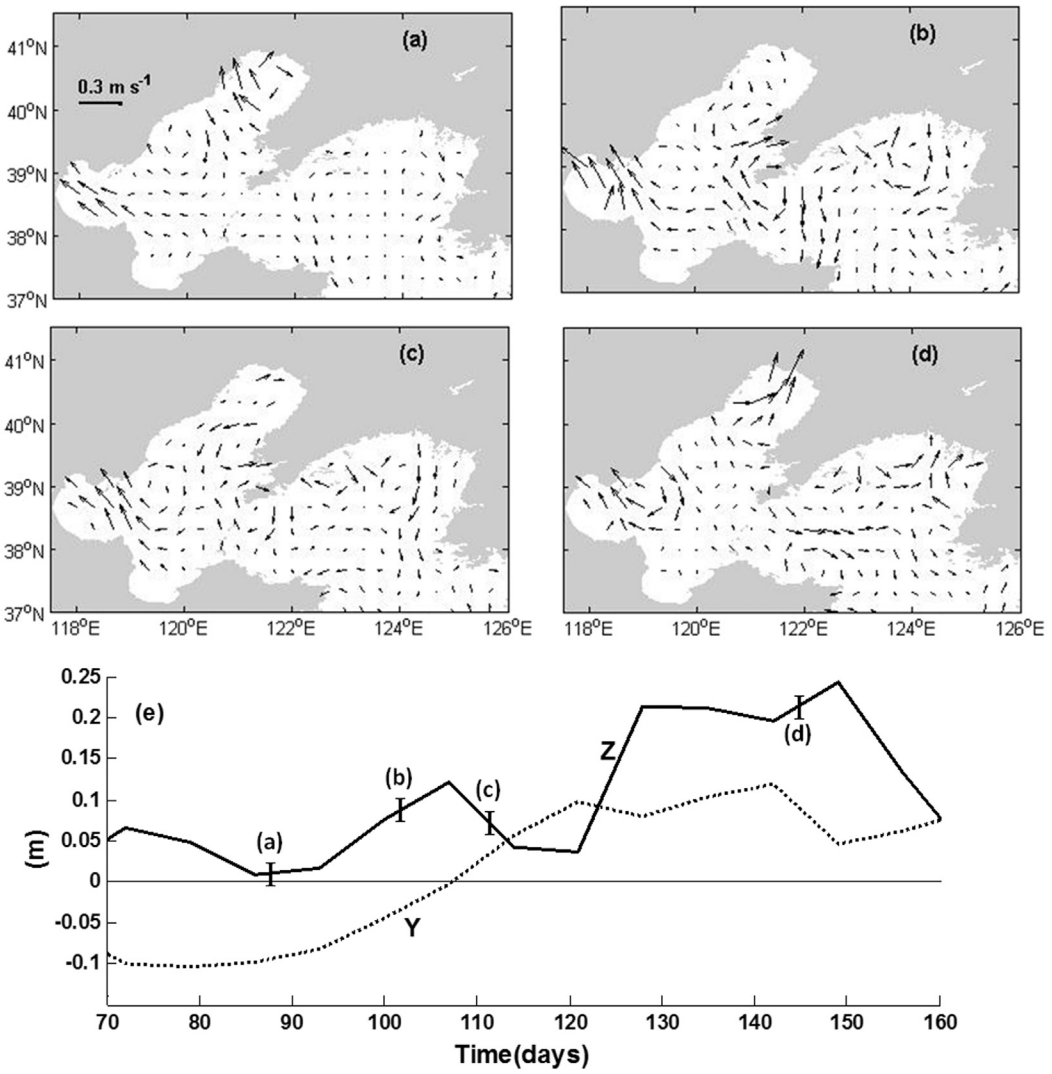

Fig. 7. Observed net surface currents averaged over 5 days and centered on (a) 28 March, 2013, (b) April 12, 2013, (c) April 22, 2013, and (d) May 27, 2013, showing water initially entering and later leaving the Bohai Sea through the Bohai Strait as a result of fluctuating MSL in the Yellow Sea. (e) shows a time series plot during that period at stations Y and Z located, respectively (see Fig. 1a), in the southern Yellow Sea, facing the East China Sea, and in the northern Yellow Sea.

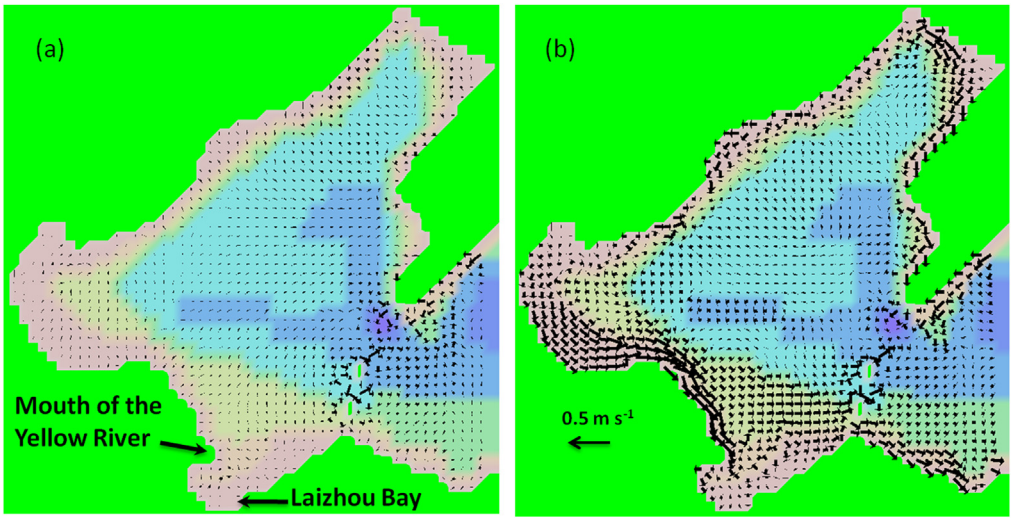

Fig. 8. Distribution of the predicted net circulation in the Bohai Sea and Bohai Strait for scenarios 1 and 7.

Table 3
The percentage of Bohai Sea water remaining in the Bohai Sea after 120 days subject to the scenarios (1–7) and mixing coefficients (A, B, C) described in Table 2, and in brackets are the estimated residence time (in years).

Scenario	A	B	C
1	91 (2.89)	90.7 (2.80)	87.4 (2.03)
2	83.7 (1.54)	83.4 (1.51)	81.6 (1.35)
3	91.6 (3.12)	91.2 (2.98)	87.9 (2.13)
4	84.1 (1.58)	83.8 (1.55)	81.9 (1.37)
5	76. (1.0)	75.8 (0.99)	75.9 (1.0)
6	75.6 (0.98)	75.6 (0.98)	75.7 (0.98)
7	63.4 (0.60)	64.5 (0.62)	67.6 (0.70)

days) waves in the China Sea, possibly generated by the meandering of the Kuroshio Current. These different forcings are non-synchronised with each other and as a result the net currents through the Bohai Strait appeared chaotic. We compared the circulation in Bohai Strait with that of other straits and we found similarities and differences, the latter being mainly the importance of forcing from far field. The net currents were the smallest (~a few cm s^{-1}) during calm weather. The wind-driven cyclonic circulation in the northern Yellow Sea generated flows across the width of the Bohai Strait. As with Luzon Strait this current meandered and a branch of the current intruded into the Bohai Strait along the deeper channel to the north. On entering the Bohai Sea this water mixed with the wind-driven coastal current there. On the south side of the Bohai Sea the wind generated a set-up ΔMSL1 and this, together with the eastward wind-driven longshore current in the southern Bohai Sea, enabled a seaward flow through the Bohai Strait, somewhat as in the Gulf of Riga. As with the Seto Inland Sea, recirculating flows occur in some embayments, e.g. Laizhou Bay. As in the Torres Strait, the islands in the Bohai strait generate mixing that retards the net flow and also help increase the width of the seaward flow zone. In addition, these flows were modulated by long waves in the Yellow Sea that created a sea-level difference ΔMSL2, additional to ΔMSL1, through the strait (Fig. 2k). The net seaward flow through the Bohai Strait was enhanced when ΔMSL2 > 0. Some of the outflow water was exported by the currents into the Yellow Sea and did not return when ΔMSL2 < 0. The

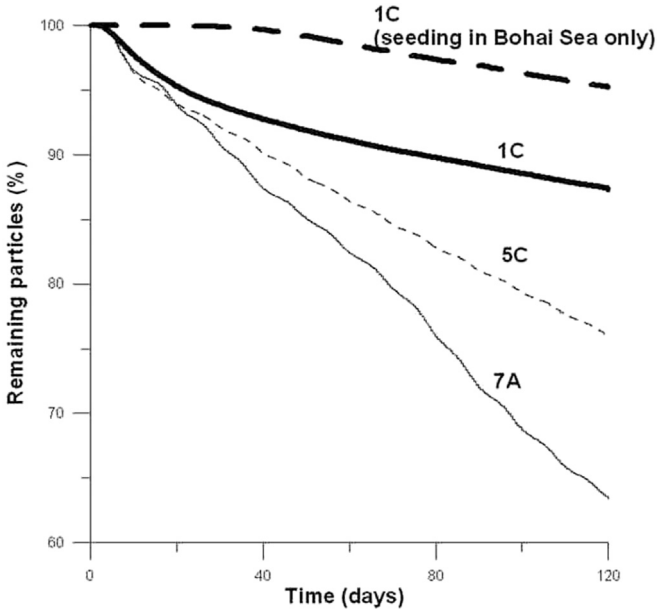

Fig. 9. Time-series plot of the predicted number of particles remaining in the Bohai Sea-Bohai Strait system for various scenarios listed in Table 2.

long waves in the Yellow Sea thus enhanced the flushing of the Bohai Sea through the Bohai Strait, and this depended on the return coefficient, i.e. the fraction of retuning water exported by long waves that returns later.

We suggest that future oceanographic models of the Bohai Sea/Bohai Strait system: (1) use a very small mesh size in the Bohai Strait so as to best simulate the effects of the islands, (2) be in 3D so as to better reproduce the summer conditions, (3) include the forcing by long waves from the China Sea, (4) be verified against the altimetry-derived current data until other current data from oceanographic moorings become available.

Acknowledgments

This study was supported by the "Strategic Priority Research Program" of the Chinese Academy of Sciences, Grant No. XDA11020401 and "Key Deployment Project" of the Chinese Academy of Sciences, Grant No. KZZD-EW-14. Eric Wolanski was supported by a Visiting Professorship of the Chinese Academy of Sciences (Grant No. 2013T2Z0033). We thank Dr. Jianhui Tang for encouragement and support. We also appreciate the OSCAR Project Office for providing the surface current data.

References

Alosairi, Y., Imberger, J., Falconer, R.A., 2011. Mixing and flushing in the persian gulf (Arabian gulf). J. Geophys. Res. 116, C03029. http://dx.doi.org/10.1029/2010JC006769.
Amiruddin, A.M., Ibrahim, Z.Z., Ismail, S.A., 2011. Water mass characteristics in the Strait of Malacca using ocean data view. Res. J. Environ. Sci. 5, 49–58.
Andutta, F.P., Ridd, P.V., Deleersnijder, E., Prandle, D., 2014. Contaminant exchange rates in estuaries—New formulae accounting for advection and dispersion. Prog. Oceanogr. 120, 139–153.
Apel, J.R., Holbrook, J.R., Liu, A.K., Tsai, J., 1985. The Sulu Sea internal solitons experiment. J. Phys. Oceanogr. 15, 1625–1651.
Armi, L., Farmer, D., 1985. The internal hydraulics of the Strait of Gibraltar and associated sills and narrows. Oceanol. Acta 8, 37–46.
Bignami, F., Salusti, E., 1990. Tidal currents and transient phenomena in the Strait of Messina: a review. The physical oceanography of sea Straits. NATO ASI Ser. 318, 95–124.
Bowden, K.F., 1956. The flow of water through the Straits of Dover, related to wind and differences in sea level. Philosophical Trans. R. Soc. Lond. A 248, 517–551.
Brinkman, R., Wolanski, E., Deleersnijder, E., McAllister, F., Skirving, W., 2002. Oceanic inflow from the coral sea into the Great Barrier reef. Estuar. Coast. Shelf Sci. 54, 655–668.
Cáceres, M., Valle-Levinson, A., Molinet, C., Castillo, M., Bello, M., Moreno, C., 2006. Lateral variability of flow over a sill in a channel of southern Chile. Ocean. Dyn. 56, 352–359.
Chang, P.-H., Guo, X., Takeoka, H., 2009. A numerical study of the seasonal circulation in the Seto Inland Sea, Japan. J. Oceanogr. 65, 721–736.
Chen, G., Hou, Y., Chu, X., 2011. Water exchange and circulation structure near the Luzon Strait in early summer. Chin. J. Oceanogr. Limnol. 29, 470–481.
Chen, M., Murali, K., Khoo, B.-C., Lou, J., Kumar, K., 2005. Circulation modelling in the strait of Singapore. J. Coast. Res. 21, 960–972.
Cheng, P., Gao, S., Boku, B., 2004. Net sediment transport patterns over the Bohai Strait based on grain size trend analysis. Estuar. Coast. shelf Sci. 60, 203–212.
Chong, V.C., King, B., Wolanski, E., 2005. Physical features and hydrography. In: Sasekumar, A., Chong, V.C. (Eds.), Ecology of Klang Strait. Faculty of Science, University of Malaya, Kuala Lumpur, pp. 1–16, 269 pp.
Cummins, P.F., 2000. Stratified flow over topography: time-dependent comparisons between model solutions and observations. Dyn. Atmos. Oceans 33, 43–72.
Fang, Y., Fang, G.H., Zhang, Q.H., 2000. Numerical simulation and dynamic study of the wintertime circulation of the Bohai Sea. Chin. J. Oceanol. Limnol. 18, 1–9.
Farmer, D., Armi, L., 1999. Stratified flow over topography: the role of small scale entrainment and mixing in flow establishment. Proc. R. Soc. Lond. A 455, 3221–3258.
Guo, X., Futamura, A., Takeoka, H., 2004. Residual currents in a semi-enclosed bay of the Seto Inland Sea, Japan. J. Geophys. Res. 109, C12008.
Hainbucher, D., Hao, W., Pohlmann, T., Sundermann, J., Feng, S., 2004. Variability of the Bohai Sea circulation based on model calculations. J. Mar. Syst. 44, 153–174.
Harvey, J.G., 1968. The flow of water through the Menai Straits. Geophys. J. R. Astronomical Soc. 15, 517–528.
Hendrawan, I.G., Asai, K., 2011. Numerical Study of tidal upwelling over the sill in the Lombok Strait (Indonesia). In: Proceedings of the Twenty-first (2011) International Offshore and Polar Engineering Conference, Maui, Hawaii, USA, June 19–24, 2011, pp. 949–956.

Hrycik, J.M., Chasse, J., Ruddick, B.R., Taggart, C.T., 2013. Dispersal kernel estimation: a comparison of empirical and modelled particle dispersion in a coastal marine system. Estuar. Coast. Shelf Sci. 133, 11–22.
Hsu, M.K., Liu, A.K., 2000. Nonlinear internal waves in the South China Sea. Can. J. Remote Sens. 26, 72–81.
Huang, D.J., Su, J.L., Backhaus, J.O., 1999. Modelling the seasonal thermal stratification and baroclinic circulation in the Bohai Sea. Cont. Shelf Res. 19, 1485–1505.
Imasato, N., Awaji, T., Kunishi, H., 1980. Tidal exchange through Naruto, Akashi and Kitan straits. J. Oceanogr. Soc. Jpn. 36, 151–162.
Ivanov, V.A., Stashchuk, N.M., Khmara, T.V., 1996. The study of the instability of currents in the Bosphorus Strait. Phys. Oceanogr. 7, 331–338.
Jakobsen, F., Hansen, I.S., Hansen, N.E.O., Østrup-Rasmussen, F., 2010. Flow resistance in the Great Belt, the biggest strait between the North Sea and the Baltic Sea. Estuar. Coast. Shelf Sci. 87, 325–332.
Kanarska, Y., Maderich, V., 2008. Modelling of seasonal exchange flows through the Dardanelles Strait. Estuar. Coast. Shelf Sci. 79, 449–458.
Kimura, S., Sugimoto, T., 2000. Two processes by which short-period fluctuations in the meander of the Kuroshio affect its countercurrent. Deep Sea Res. Part 1: Oceanogr. Res. Pap. 47, 745–754.
Li, G.S., Wang, H.L., Li, B.L., 2005. A model study on seasonal spatial-temporal variability of the Lagrangian residual circulations in the Bohai Sea. J. Geogr. Sci. 15, 273–285.
Liu, Z., Wang, H., Guo, X., Wang, Q., Gao, H., 2012. The age of Yellow River water in the Bohai Sea. J. Geophys. Res. 117, C11006.
Lu, J., Qiao, F.L., Wang, X.H., Wang, Y.G., Teng, Y., Xia, C.S., 2011. A numerical study of transport dynamics and seasonal variability of the Yellow River sediment in the Bohai and Yellow seas. Estuar. Coast. Shelf Sci. 95, 39–51.
Medeiros, C., Kjerfve, B., 1988. Tidal characteristics of the Strait of Magellan. Cont. Shelf Res. 8, 947–960.
Melet, A., Gourdeau, L., Verron, J., Djath, B., 2013. Solomon Sea circulation and water mass modifications: response at ENSO timescales. Ocean. Dyn. 63, 1–19.
Ningshi, N.S., Yamashita, T., Aouf, L., 2000. Three-dimensional simulation of water circulation in the Java sea: Influence of wind waves on surface and bottom stresses. Nat. Hazards 21, 145–171.
Pishchal'nik, V.M., Arkhipkin, V.S., Leonov, A.V., 2010. On water circulation in Tatar Strait. Water Resour. 37, 759–772.
Pous, S.P., Carton, X., Lazure, P., 2004. Hydrology and circulation in the Strait of Hormuz and the Gulf of Oman—Results from the GOGP99 Experiment: 1. Strait of Hormuz. J. Geophys. Res. 109, 2156–2202.
Pratt, L.J. (Ed.), 1990. The Physical Oceanography of Sea Straits. NATO ASI Series, vol. 318, 587 pp.
Qiu, B., Toda, T., Imasato, N., 1990. On Kuroshio front fluctuations in the East China Sea using satellite and in situ observational data. J. Geophys. Res. 95, 18191–18204.
Reynolds, R.M., 1993. Physical oceanography of the gulf, Strait of Hormuz, and the Gulf of Oman—Results from Mt. Mitchell expedition. Mar. Pollut. Bull. 27, 35–59.
Rizal, S., Damm, P., Wahid, M.A., Sundermann, J., Ilhamsyah, Y., Iskandar, T., Muhammad, 2012. General circulation in the Malacca Strait and Andaman Sea and Andaman Sea: a numerical model study. Am. J. Environ. Sci. 8, 479–488.
Sennikovs, J., Bethers, U., 2000. Shallow water calculation of circulation for Gulf of Riga. Finn. Mar. Res. Ser.
Spagnol, S., Wolanski, E., Deleersnijder, E., Brinkman, R., McAllister, F., Cushman-Roisin, B., Hanert, E., 2002. An error frequently made in the evaluation of advective transport in two-dimensional Lagrangian models of advection-diffusion in coral reef waters. Mar. Ecol. Prog. Ser. 235, 299–302.
Swaney, D.P., Smith, S.V., Wulff, F., 2011. The LOICZ biogeochemical modeling protocol and its application to estuarine ecosystems. Treatise Estuar. Coast. Sci. 9, 136–159.
Uncles, R.J., Torres, R., 2013. Estimating dispersion and flushing time-scales in a coastal zone: application to the Plymouth area. Ocean Coast. Manag. 73, 3–12.
Wang, H., Wang, A., Bi, N., Zeng, X., Xiao, H., 2014. Seasonal distribution of suspended sediment in the Bohai Sea, China. Cont. Shelf Res. 90, 17–32.
Wolanski, E., 2007. Estuarine Ecohydrology. Elsevier, Amsterdam, p. 157.
Wolanski, E., Lambrechts, J., Thomas, C., Deleersnijder, E., 2013. The net water circulation through Torres Strait. Cont. Shelf Res. 64, 66–74.
Yu, L., Weller, R.A., 2007. Objectively analyzed air-sea heat fluxes for the global ice-free oceans (1981–2005). Bull. Am. Meteorol. Soc. 88, 527–539.